

Hypoxia induces genomic DNA demethylation through the activation of HIF-1 α and transcriptional up-regulation of MAT2A in hepatoma cells

Quanyan Liu^{1#}, Li Liu^{1#}, Yuhong zhao², Jun Zhang¹, Dongfeng Wang¹, Jiwei Chen¹,
Yueming He¹, Jianguo Wu³, Zhonglin Zhang¹ and Zhisu Liu^{1*}

¹Department of General Surgery, Zhongnan Hospital, Wuhan University, Wuhan 430071, China

²Department of Pharmacology, Guangdong Pharmaceutical University, Guangzhou 510006, China

³State Key Laboratory of Virology and College of Life Sciences, Wuhan University, Wuhan 430072, China.

contributed equally

* Corresponding author: Department of General Surgery, Zhongnan Hospital, Wuhan University, Wuhan 430071, China; Tel.: +86-27-68713007; Fax: +86-27-87330795;
E-mail: spss2005@126.com

Running title:

HIF-1 α induces genomic DNA demethylation via MAT2A

Keywords:

DNA methylation; Hypoxia-inducible factor 1; Methionine adenosyltransferase 2A; Hepatocellular carcinoma; S-adenosylmethionine.

Abstract Hypoxia-inducible factor 1 (HIF-1) emerges as a crucial player in tumor progression. However, its role in hepatocellular carcinoma (HCC), especially its relation with global DNA methylation patterns in HCC under hypoxic tumor microenvironment is not completely understood. Methionine adenosyltransferase 2A (MAT2A) maintains the homeostasis of S-adenosylmethionine (SAM), a critical marker of genomic methylation status. In this study we investigated the link between HIF-1 α and MAT2A as a mechanism responsible for the change in genomic DNA methylation patterns in liver cancer under hypoxia conditions. Our results demonstrated that hypoxia induces genomic DNA demethylation in CpG islands by reducing the steady-state SAM level both in vitro and in vivo. In addition, HIF-1 α and MAT2A expression is correlated with tumor size and TNM stage of liver cancer tissues. We further demonstrated that hypoxia-induced MAT2A expression is HIF-1 α dependent and requires the recruitment of p300 and HDAC1. We also identified an authentic consensus HIF-1 α binding site in MAT2A promoter by site-directed mutagenesis, electrophoretic mobility shift assay and chromatin immunoprecipitation assay. Taken together, we show for the first time that hypoxia induces genomic DNA demethylation through the activation of HIF-1 α and transcriptional up-regulation of MAT2A in hepatoma cells. These findings provide new insights into our understanding of the molecular link between genomic DNA methylation and tumor hypoxia in HCC.

Introduction

The high proliferation of tumor cells induces local hypoxia inside the tumor, recent evidence suggests that hypoxia is crucially involved in tumor progression and angiogenesis [1, 2]. Notably, hypoxia modulates the malignant phenotypes of tumor cells via hypoxia-inducible factor 1 (HIF-1), a crucial transcription factor that regulates the expression of numerous target genes [3-5]. Nevertheless, it remains unclear whether HIF-1 upregulation is involved in the initiation or the progression stages of hepatocarcinogenesis.

Recent studies have shown hypoxia-induced genome-wide effects in liver tumor [6-8]. Such hypoxic changes may be due to alterations in epigenetic profiles. DNA methylation is now recognized as a critical epigenetic mark and alterations in DNA methylation is involved in multistage of HCC, even in the early precancerous stages [9]. Specially, in premalignant conditions such as dysplastic nodules or cirrhotic liver, the promoters of TSGs including E-cadherin, glutathione S-transferase P1, and p16Ink4a are frequently hypermethylated [10]. In contrast, the genome-wide hypomethylation in HCC was shown as an ongoing process throughout the lifetime of the tumor cells rather than a historical event occurring in precancer stages, but how this change is associated with genomic instability or the activation of proto-oncogenes in HCC remains elusive [11].

S-adenosylmethionine (SAM) is a major biological methyl donor. SAM-dependent methylation has been shown to be central to many biological processes and the steady-state SAM level has been accepted as a critical marker of the genomic methylation status [12, 13]. In hepatocytes, SAM level is related to the differentiation

status of the cells, being high in quiescent hepatocytes and low in proliferating hepatocytes [14-16]. SAM is synthesized from methionine and ATP in a reaction catalyzed by methionine adenosyltransferase (MAT). In mammals MAT is encoded by two genes, MAT1A and MAT2A. A switch of MAT expression from MAT1A to MAT2A is frequently observed during malignant liver transformation, and this alteration plays an important pathogenetic role in facilitating liver cancer progression [17-19].

Nevertheless, the influence of the hypoxic tumor microenvironment on DNA methylation patterns in HCC is not completely understood. Therefore, in this study we investigated the potential interaction between HIF-1 α and MAT2A as a mechanism responsible for the change in genomic DNA methylation patterns in liver cancer under hypoxia conditions. We identified MAT2A as a novel target gene that is transcriptionally regulated by HIF-1 α , and provided evidence that hypoxia regulates genomic DNA methylation through activation of HIF-1 α and transcriptional up-regulation of MAT2A in hepatoma cells. Thus our data establish a molecular link between genomic DNA methylation and hypoxia in liver cancer.

Materials and Methods

Cell culture and transfection

Hepatoma cell lines BEL-7404, Hep3B and HepG2 were obtained from the Cell Bank of the Chinese Academy of Sciences (Shanghai, China) where they were characterized by mycoplasma detection, DNA-Fingerprinting, isozyme detection and

cell vitality detection. These cell lines were immediately expanded and frozen such that they could be restarted every 3 to 4 months from a frozen vial of the same batch of cells. All cells were cultured in the recommended media supplemented with 10% (v/v) fetal bovine serum, 100 units/ml penicillin, and streptomycin at 37 °C in an incubator with 5% CO₂. The current authors have not independently tested and authenticated these cells. Routine testing for Mycoplasma infection was done using the MycoTect kit (Invitrogen). For hypoxia experiments, the oxygen partial pressure was lowered to 0.9 kPa (1% O₂ by volume). Transfection was performed using LipofectAMINE™ 2000 (Invitrogen). MAT2A promoter region (-2403/+102) was PCR amplified from human genomic DNA and cloned into pGL3-Basic vector and co-transfected with HIF-1 α expression vector (pCMV-HIF-1 α , OriGene) or pCMV empty vector and an internal control pRL-SV40 plasmid (Promega). For MAT2A promoter deletion constructs, pGL3 promoter vectors containing different fragments of MAT2A promoter (-2403/+102, -913/+102, -411/+102, or -205/+102) were transfected. Luciferase activities were measured using the Dual-Luciferase system (Promega) and an Infinite™ F200 luminometer (TECAN). For site-directed mutagenesis, the putative HRE motif was mutated using the QuickChange site-directed mutagenesis kit (Stratagene), from 5'-ATCCCCC**ACGT**CTCCTCG-3' to 5'-ATCCCCC**TAGT**CTCCTCG-3'.

HCC xenograft model

Female BALB/c nude mice 4-5 weeks old were obtained from the Shanghai

Experimental Animal Center of the Chinese Academy of Sciences (Shanghai, China). All procedures were performed according to institutional guidelines. $1-2 \times 10^6$ hepatoma cells were subcutaneously injected into the flank of female nude mice. Tumor growth was monitored using Vernier calipers, and the volume was calculated using the standard formula (length \times width² \times 0.5). Tissues were harvested once the tumor volume was approximately 100–200 mm³. Tumors were removed and cut into pieces that were then snap-frozen in cryomatrix and stored at -80°C.

Endogenous C-5 DNA methyltransferase (C-5 MTase) activity

DNA MTase activity was determined as described previously [20]. 20 μ l reaction mixture containing cell homogenates (5 μ g protein), poly (dI-dC) (0.25 μ g) and 11.1×10^{10} μ Bq of [methyl ³H] SAM was incubated at 37°C for 2 h. The DNA was purified using the E.Z.N.A. Cycle-Pure kit, and purified genomic DNA was spotted onto Whatman GF/C filter disc, dried at 80°C for 5 min and counted using a scintillation counter (1600TR Packard Instrument Comp). Results were expressed as dnm/ μ g protein.

Methylation-dependent restriction analysis

The methyl-accepting capacity of genomic DNA was measured as the loss of unmethylated cytosine after genomic DNA was digested with methylation-sensitive endonucleases as described previously [21]. 5 μ g purified genomic DNA was digested with HpaII and BssHIII overnight. Samples of undigested genomic DNA served as

controls. The digested and undigested genomic DNA samples were purified with the E.Z.N.A. Cycle-Pure kit for the DNA methyl-accepting capacity assay as follows: purified genomic DNA (0.5 μ g), bacterial SssI methylase (2 U) and [methyl- 3 H] SAM (3 Bq per sample) were incubated in buffer containing 50 mM NaCl, 10 mM Tris-HCl, pH 8.0, and 10 mM EDTA for 2 h at 37°C. Then, 25 μ l aliquots were taken from each reaction mixture, applied to GF/C filter discs, and counted in scintillation counters. The results were expressed as [methyl- 3 H] incorporation/0.5 μ g DNA.

Analysis of genomic DNA methylation status

Global DNA methylation was determined as previously described [22, 23]. 3 μ g purified DNA was incubated with 3 units HpaII or SssI and 2.5 μ Ci of [methyl- 3 H] SAM in 50 μ l buffer. The mixture was incubated overnight at 4°C, and unlabeled SAM was then added. The total SAM concentration was 160 μ M for SssI and 80 μ M for HpaII. After incubation at 37°C for 3 h, five volumes of ice-cold trichloroacetic acid (TCA) were added to the mixture. The mixture was centrifuged, and the pellet was washed with TCA and centrifuged at 10,000 g for 30 min. Finally, the pellet was dissolved in 50 μ l 0.1 N NaOH and counted for radioactivity.

Assay of S-adenosylmethionine (SAM) and S-adenosylhomocysteine (SAH)

The assay was performed using reversed-phase high-performance liquid chromatography (HPLC) based on previously described procedures [18, 24]. SAM and SAH standards were dissolved in water at 1 mM and diluted in 0.4 M HClO₄ to

the final concentrations used for HPLC analysis. A total of 25 μ l standard injected solution containing 50-11000 pmol were added to the HPLC for making a standard curve.

Patients and tissue specimens

A total of 58 cases of surgically resected HCCs were collected from Zhongnan Hospital, Wuhan University, between January 2009 and January 2010. No chemotherapy or radiation therapy was performed before tumor excision. Both the tumors and the corresponding peritumoral non-cancerous tissues for each case were selected. Matched normal human liver tissues were obtained from liver trauma patients undergoing partial hepatectomy. Written informed consent was obtained from each patient. The study protocol was approval by the local ethics committee.

Immunohistochemistry

Representative tissues were selected and sectioned in 4 μ m thick. The tissue samples were fixed by immersion in buffered formalin and embedded in paraffin according to standard procedures. All specimens stained for HIF-1 α and MAT2A were scored by two independent investigators who were blinded to the test groups. HIF-1 α and MAT2A immunostaining was scored based on the percentage of cells that had positive staining in the cytoplasm. Slides were graded as follows: - (0 to 10% cells stained), + (10 to 50% cells stained), or ++ (>50% cells stained).

Immunofluorescence experiments

Cells were seeded on coverslips in a 6-well plate and grown to 70-80% confluence. After exposure to hypoxia for 24 h, the medium was aspirated, and cells were washed twice with PBS. Cells were fixed in methanol for 30 min at -20°C, then incubated with HIF-1 α antibody (Santa Cruz Biotechnology) for 1 h at 37°C, followed by incubation with FITC labeled secondary antibody (1: 2000 dilution in PBS) for 1 h at 37°C. Nuclei were counterstained with Propidium Iodide. Dual-color fluorescence images were captured using a digital camera and confocal microscope (Olympus FluoView FV300, Japan).

Western blotting

Nuclear and cytoplasmic protein extracts were prepared from transfected cells. Protein (30 μ g) from each sample was examined using 10% SDS-PAGE and then electrotransferred to nitrocellulose membranes. The membranes were subjected to Western blot analysis using antibodies against HIF-1 α (Santa Cruz), MAT2A, DNMT1, DNMT3 α and DNMT3 β (Abcam) following standard procedures, and developed using ECL kit (Amersham).

Electrophoresis mobility shift assay (EMSA)

Oligonucleotide probes were purchased from Life Technologies (Life Technologies, Gaithersburg, MD), the sequence (coding strand) of the wild-type probe was 5'-GAGCAATCCCCC $\boxed{\text{ACGT}}$ CTCCTCG-3' and that of the mutant probe was

5'-GAGCAATCCCCC**TAGT**CTCCTCG-3'. Radioactive oligonucleotides were generated by 5' end labeling using T4 polynucleotide kinase (Amersham). Binding reactions were performed with 5 mg nuclear extracts, 0.1 mg denatured calf thymus DNA and 1 ng radiolabeled probe (10,000 cpm). Supershift experiments were performed in the presence of a monoclonal HIF-1 α antibody (Novus). Electrophoresis was performed on a 5% nondenaturing PAGE, and the gels were dried for autoradiograph.

Chromatin immunoprecipitation (ChIP) and re-ChIP assays

ChIP assays were performed with a rabbit antibody against human HIF-1 α (Abcam) using a ChIP assay kit (Millipore), and Re-ChIP assay was performed using a procedure described by Metivier et al. [25]. Briefly, HIF-1 α ChIP complexes were eluted by incubation with 25 μ l 10 mM dithiothreitol (Calbiochem) for 30 min at 37°C. After centrifugation, the supernatant was diluted in a re-ChIP buffer (20 mM Tris-HCl, 150 mM NaCl, 2 mM EDTA and 1% Triton X-100, pH 8.0). The diluted complexes were then subjected to immunoprecipitation using mouse anti-human p300 antibody (BD Pharmingen) or rabbit anti-human HDAC1 antibody (Cell Signaling Technology). The immunoprecipitated chromatin was analyzed in triplicate by PCR using the primers AGTGCGGCCAACGCCG (forward) and AAGTTGGGCGCCGCTTGGA (reverse) for human MAT2A promoter.

Statistical analysis

Statistical analysis were performed using SPSS 15.0 statistics software (SPSS, Chicago, IL, USA). Data were expressed as mean \pm standard deviation ($X \pm SD$). Student's unpaired t-test was used to compare two groups. The Spearman rank correlation test was used to determine correlations between variables. $P < 0.05$ was considered significant.

Results

Hypoxia induces genomic DNA hypomethylation in CpG islands in Hep3B cells

We examined the effect of hypoxia on DNA methylation in hepatoma cells. The levels and patterns of DNA methylation were determined by measuring endogenous C-5 DNA methyltransferase (C-5 MT-ase) activity and the methyl-accepting capacity of undigested genomic DNA. The results showed that hypoxia up-regulates the activity of C-5 MT-ase in Hep3B cells compared to normoxia group, with maximum activity shown 24 h after hypoxia ($P < 0.001$, Fig. 1A). In addition, the number of genomic DNA methylation sites available for SssI methylase was increased significantly under hypoxic conditions compared to normoxia ($P < 0.001$) and reached the peak 24 h after hypoxia (Fig. 1B). The genomic DNA isolated from the cells exposed to hypoxia exhibited 1.38, 1.59 and 1.43 fold more methyl acceptance than normoxia-treated cells 12 h, 24 h and 36 h after hypoxia, respectively. These data demonstrated that hypoxia induced a demethylation process in genomic DNA.

Because methylation-dependent restriction endonucleases can cut specific CG sequences but not methylated ^mCG, digestion with HpaII or BssHII results in the

destruction of corresponding CG loci and loss of the potential methylation-accepting sites. The results showed an increase in the methyl-accepting capacity of genomic DNA that was not digested by restriction endonucleases in hypoxia groups. However, the digestion of DNA by methylation-dependent endonucleases led to a decrease in the methyl-accepting capacity of genomic DNA. A greater decrease in methylation-accepting capacity was noted in groups digested with BssHIII, being 48.1%, 71.4%, and 45.9% compared to undigested DNA 12 h, 24 h and 36 h after hypoxia, respectively. The methylation-accepting capacity of the HpaII-digested groups declined 15.9%, 26.1% and 12.4% compared to undigested DNA 12 h, 24 h and 36 h after hypoxia, respectively. Thus, the results of the methylation-dependent restriction analysis indicated that hypoxia induced decreased methylation in hepatoma cell genomic DNA with a bias for CpG islands (GC⁺GCGC sequences) but not C⁺CGG sequences.

Hypoxia reduces the SAM/SAH ratio in Hep3B cells

The ratio of SAM/SAH is a predictor of methylation. Therefore, we examined the changes in SAM, SAH and MTA levels in Hep3B cells exposed to hypoxia (1% oxygen). As shown in Supplemental Table 1, SAM level in cultured Hep3B cells under hypoxic conditions was decreased significantly compared to normoxic cells ($P < 0.001$), reaching the lowest point 24 h after hypoxia. The ratio of SAM to SAH decreased in parallel with the SAM level, whereas the SAH and MTA levels remained relatively unchanged.

Hypoxia induces genomic DNA hypomethylation in vivo

To demonstrate the effect of hypoxia on DNA methylation in vivo, we established xenograft tumors in nude mice. All liver cancer cell lines exhibited higher HIF-1 α and MAT2A expression in the xenograft tumors than cultured in vitro, indicating that xenograft tumor growth could mimic in vivo hypoxic microenvironment and induce HIF-1 α and MAT2A overexpression (Fig. 2A). Next, we investigated the changes in SAM and SAH levels after xenograft tumor formation in vivo, and found that all liver cancer cell lines (Bel-7402, HepG2 and Hep3B) showed a reduction in SAM content when grown as xenografts compared to cultured in vitro ($p < 0.05$, Fig. 2B). In contrast, the SAH level observed in xenografts was not significantly different from the control culture (Fig. 2C). Furthermore, DNA methylation status was evaluated by the radioactivity incorporated from labeled SAM in the xenograft tumors and compared to levels in the same cancer cell lines in vitro. HpaII-mediated incorporation of radioactivity (CCGG specificity) in DNA isolated from hypoxic xenograft was only slightly higher than that from the cell lines ($p > 0.05$; Fig. 2D). However, SssI-mediated incorporation of radioactivity (CpG specificity) in DNA isolated from hypoxic xenografts was higher in xenografts than in the cell lines (Fig. 2E). Taken together, these results demonstrate that hypoxia reduces the SAM level and induces genomic DNA hypomethylation in vivo.

The expression of HIF-1 α and MAT2A is correlated under hypoxic conditions

To investigate the clinical significance of the link between hypoxia and DNA methylation, we examined HIF-1 α and MAT2A expression in 58 paired liver cancer tissues and corresponding peritumoral tissues by immunohistochemical staining. Representative results showed that HIF-1 α expression was high in liver cancer tissue but was low in the corresponding peritumoral tissue and undetected in normal liver tissue (Fig. 3A). Similar results were obtained for MAT2A (Fig. 3B). The potential correlation between the expression of HIF-1 α and MAT2A was further analyzed (Supplemental Table 2). Spearman analysis showed that the expression of HIF-1 α was positively correlated with MAT2A ($r = 0.752$, $P < 0.001$) in liver cancer tissues. Furthermore, we analyzed the clinicopathologic characteristics of human liver samples and found that the expression of HIF-1 α and MAT2A was correlated with tumor size and TNM stage (supplemental Table 3).

To further confirm the correlation of HIF-1 α with MAT2A under hypoxic conditions, we performed luciferase assay and found that MAT2A promoter activity was notably increased in Hep3B cells under hypoxic conditions (Fig. 3B). Western blot analysis also revealed the positive correlation between HIF-1 α and MAT2A expression in Hep3B cells after hypoxic treatment (Fig. 3C). In addition, we determined whether hypoxia has an effect on the expression level of the major methyltransferases DNMT1, DNMT3a, and DNMT3b. The results showed that hypoxia upregulated the expression of DNMT1 and DNMT3 α but not DNMT3 β in Hep3B cells (Fig. 3D).

To address the role of HIF-1 α in the regulation of MAT2A expression in

hypoxia, we employed siRNA to knockdown HIF-1 α and found that this could block MAT2A expression at the protein level induced by either hypoxia or treatment with CoCl₂, a chemical inducer of HIF-1 α (Fig. 3E). Collectively, these data suggest that HIF-1 α mediates hypoxia-induced MAT2A expression.

HIF-1 α overexpression induces MAT2A promoter activity in normoxic Hep3B cells

To provide further evidence that MAT2A is a direct target gene of HIF-1 α , we transfected HIF-1 α expression vector into Hep3B cells for the overexpression of HIF-1 α under normoxic condition (Fig. 4A). We located one putative HIF-1 α binding site at the -281/-261 region in human MAT2A promoter (Fig. 4B). Luciferase assay showed that HIF-1 α overexpression significantly increased the luciferase activities driven by the pGL3-MAT2A (0.5 kb) promoter but not by the pGL3-MAT2A (0.25 kb) promoter (Fig. 4C). We then truncated the promoter fragment and demonstrated that that -410/-204 fragment contains the putative HIF-1 α binding motif (Fig. 4D). Mutation of the putative HIF-1 α binding motif (ATCCCCC $\overline{\text{ACGT}}$ CTCCTCG) abolished the induction of luciferase activity in HIF-1 α overexpressing cells (Fig. 4E). Taken together, these data suggest that MAT2A is a direct target of HIF-1 α .

HIF-1 α binds the consensus HRE in MAT2A promoter in hypoxic Hep3B cells

By EMSA assay we observed a supershift obtained by co-incubation with monoclonal HIF-1 α antibody and the absence of binding in a 30-fold excess of

unlabeled wild-type or labeled mutant oligonucleotide, demonstrated the specificity of HIF-1 α binding. The specificity was further confirmed by a non-specific competition assay with a 30-fold excess of unlabeled mutated oligonucleotide, which did not cause any difference in signal intensity (Fig. 5A). ChIP assay demonstrated a significant increase in HIF-1 α binding to MAT2A promoter in hypoxic Hep3B cells (Fig. 5B). In addition, by immunofluorescence and cell fractionation we demonstrated that HIF-1 α was translocated into the nucleus in Hep3B cells under hypoxic conditions (Fig. 5C, D). Taken together, these results suggest that hypoxia induces the nuclear translocation of HIF-1 α , where it could bind directly to the consensus HRE in MAT2A promoter in Hep3B cells.

HIF-1 α mediated transcriptional activation of MAT2A requires the recruitment of co-activators HDAC1 and p300

To test whether HDAC1 and p300 co-activators are involved in MAT2A expression regulated by HIF-1 α , we employed inhibitors of HDAC (i.e., TSA) or p300 (i.e., chetomin) and found that both treatments significantly inhibited hypoxia-induced MAT2A expression in Hep3B cells (Fig. 6A and B).

To further prove the interaction of HDAC1 and p300 with MAT2A promoter under hypoxic conditions, re-ChIP assays were performed to confirm the binding of HDAC1 and p300 to HIF-1 α transcription complex. Hypoxic Hep3B cells showed a high level of HDAC1 and p300 binding to MAT2A promoter compared to the control. TSA and chetomin treatment of hypoxic Hep3B cells caused a significant reduction in

HDAC1 and p300 binding to the promoter, respectively, as well as a reduction of the binding of HIF-1 α to MAT2A promoter (Fig. 6C).

Discussion

The liver is one of the organs in which hypoxia regulate gene expression under normal physiological conditions and in diseases such as cirrhosis and cancer [26-28]. In addition, hypoxic conditions may disrupt DNA methylation patterns, providing a potential link between the extracellular environment, epigenetic alterations and cancer progression [29, 30]. Thus the progression of HCC may be influenced by local epigenetic alterations under hypoxic microenvironmental conditions, leading to inappropriate silencing and activation of genes involved in cancer.

In this study we aimed to examine the linkage between abnormal DNA methylation in liver cancer and hypoxic microenvironmental conditions. We observed that hypoxia up-regulated the activity of endogenous C-5 DNA methyltransferase activity in Hep3B cells accompanied by the changes in the methylation status of genomic DNA, demonstrating a hypoxia-induced demethylation process. To elucidate the mechanism underlying the effect of hypoxia on DNA methylation in hepatoma cells, we performed methylation-dependent restriction analysis and found that hypomethylation in hepatoma cell genomic DNA in hypoxia had a sequence bias for the BssHII cutting locus, suggesting that hypoxia preferentially induces demethylation in CpG islands (GC'GCGC sequences) but not in C'CGG sequences.

Because methylation of DNA may be affected by a limited availability of SAM

or an increase in SAH, the ratio of SAM/SAH, also termed methylation potential (MP), is often a predictor for methylation [7, 31]. We demonstrated that SAM level was significantly decreased in Hep3B cells cultured under hypoxic conditions compared to normoxic cells. The ratio of SAM to SAH was decreased in parallel, but SAH and MTA levels remained relatively unchanged. However, Hermes et al. [32] observed that hypoxia leads to increased SAM and decreased SAH levels in HepG2 cells. This difference may be due to alterations in the cell density of cultured cells [33].

To confirm our in vitro results in an in vivo situation, we investigated the changes in SAM and SAH levels in xenograft tumors. All liver cancer cell lines showed a reduction in their SAM content when grown as xenografts compared to control cultures. However, the SAH level remained relatively unchanged. These results are in agreement with the findings of Chawla et al. [24]. These results indicate that a limited availability of SAM in hypoxic xenografts probably increases the unmethylated sites of DNA.

SAM is an abundant methyl donor in the metabolism and is involved in more than 100 methyl transfer reactions, including DNA methylation. It is synthesized from methionine and ATP by the enzyme methionine adenosyltransferase (MAT). MAT expression is characterized by a switch from MAT1A to MAT2A during malignant liver transformation, which plays an important pathogenetic role in liver cancer [34-36]. Therefore, it is important to study the correlation between the expression of HIF-1 α and MAT2A. In this study, Spearman analysis showed that the expression of

HIF-1 α was positively correlated with MAT2A in liver cancer tissues. Luciferase assay showed that MAT2A expression was notably increased under hypoxic conditions and HIF-1 α mediated the hypoxia-induced expression of MAT2A.

To illustrate the direct binding of HIF-1 α to MAT2A promoter, HIF-1 α binding to the consensus HRE sequence at -275 to -271 bp within MAT2A promoter was examined by EMSA and ChIP assays. Based on the results, we conclude that MAT2A is a novel target gene that is transcriptionally regulated by HIF-1 α . We further explored the transactivation mechanism of HIF-1 α mediated MAT2A expression and found that the coactivators HDAC1 and p300 are required for the formation of HIF-1 α transcription complex to activate MAT2A expression.

The MAT2A-encoded protein is the only SAM-synthesizing enzyme in the neoplastic liver because liver-specific MAT1A-encoded isoenzymes that are expressed in hepatocytes are absent in the neoplastic liver. This is the first study to demonstrate that hypoxia alters DNA methylation patterns in liver cancer through the reduction of the steady-state SAM level, although we currently have no information about how MAT2A decreases intracellular SAM level. One possible explanation is that SAM is consumed for polyamine biosynthesis. Another possibility is the known differences in the kinetic parameters of different MAT isoforms for methionine. Taken together, our study reveals new mechanisms for the regulation of DNA methylation patterns in hypoxic tumor microenvironments. We propose that in liver cancer, hypoxia activates MAT2A expression through HIF-1 α , which results in the increase in MAT II enzyme activity and a decrease in SAM production, thus inducing

genomic DNA demethylation.

Disclosure of Potential Conflicts of Interest

No potential conflicts of interest were disclosed.

Acknowledgments

We appreciate the suggestion and editorial assistance of Dr. Yingqun Wang.

Grant Support

Natural Science Foundation of China (Nos. 30730001 and 30872491), National Mega Project on Major Drug Development (No. 2009ZX09301-014), and Natural Science Foundation of Hubei Province (No. 2009CDB292).

References

- [1] Pouyssegur J, Dayan F, Mazure NM. Hypoxia signalling in cancer and approaches to enforce tumour regression. *Nature*. 2006; 441:437–43.
- [2] Rosmorduc O, Housset C. Hypoxia: a link between fibrogenesis, angiogenesis, and carcinogenesis in liver disease. *Semin Liver Dis* .2010 ; 30:258-70.
- [3] Huang LE, Bindra RS, Glazer PM, Harris AL. Hypoxia-induced genetic instability—A calculated mechanism underlying tumor progression. *J Mol Med*. 2007; 85:139–48.
- [4] Kim KW, Bae SK, Lee OH, Bae MH, Lee MJ, Park BC ,et al. Insulin-like growth factor II induced by hypoxia may contribute to angiogenesis of human hepatocellular carcinoma. *Cancer Res*. 1998; 58: 348–51.

- [5] Mylonis I, Lakka A, Tsakalof A, Simos G. The dietary flavonoid kaempferol effectively inhibits HIF-1 activity and liver cancer cell viability under hypoxic conditions. *Biochem Biophys Res Commun*. 2010; 398:74-8.
- [6] Menrad H, Werno C, Schmid T, Copanaki E, Deller T, Dehne N, et al. Roles of hypoxia-inducible factor-1alpha (HIF-1alpha) versus HIF-2alpha in the survival of hepatocellular tumor spheroids. *Hepatology*. 2010 ; 51:2183-92
- [7] Dai CX, Gao Q, Qiu SJ, Ju MJ, Cai MY, Xu YF, et al. Hypoxia-inducible factor-1 alpha, in association with inflammation, angiogenesis and MYC, is a critical prognostic factor in patients with HCC after surgery. *BMC Cancer*. 2009; 9:2407-18
- [8] Van Malenstein H, Gevaert O, Libbrecht L, Daemen A, Allemeersch J, Nevens F, et al. A Seven-Gene Set Associated with Chronic Hypoxia of Prognostic Importance in Hepatocellular Carcinoma. *Clin Cancer Res*. 2010 ; 16:4278-88.
- [9] Kanai Y. Genome-wide DNA methylation profiles in precancerous conditions and cancers. *Cancer Sci*. 2010;101:36-45.
- [10]Tischhoff I, Tannapfe A. DNA methylation in hepatocellular carcinoma. *World J Gastroenterol*. 2008; 14:1741-8.
- [11]Lin CH, Hsieh SY, Sheen IS, Lee WC, Chen TC, Shyu WC, et al. Genome-wide hypomethylation in hepatocellular carcinogenesis. *Cancer Res*. 2001;61:4238-43.
- [12]Lu SC, Mato JM. S-Adenosylmethionine in cell growth, apoptosis and liver cancer. *J Gastroenterol Hepatol*. 2008;23 Suppl 1:S73-7.
- [13]Lu SC, Mato JM. Role of methionine adenosyltransferase and

- S-adenosylmethionine in alcohol-associated liver cancer. *Alcohol*. 2005; 35:227-32.
- [14] Pañeda C, Gorospe I, Herrera B, Nakamura T, Fabregat I, Varela-Nieto I. Liver cell proliferation requires methionine adenosyltransferase 2A mRNA up-regulation. *Hepatology*. 2002; 35:1381-91.
- [15] García-Trevijano ER, Latasa MU, Carretero MV, Berasain C, Mato JM, Avila MA. S-adenosylmethionine regulates MAT1A and MAT2A gene expression in cultured rat hepatocytes: a new role for S-adenosylmethionine in the maintenance of the differentiated status of the liver. *FASEB J*. 2000; 14:2511-18.
- [16] Mato JM, Corrales FJ, Lu SC, Avila MA. S-Adenosylmethionine: a control switch that regulates liver function. *FASEB J*. 2002; 16:15-26.
- [17] Wang Q, Liu QY, Liu ZS, Qian Q, Sun Q, Pan DY. Inhibition of hepatocellular carcinoma MAT2A and MAT2beta gene expressions by single and dual small interfering RNA. *J Exp Clin Cancer Res*. 2008; 27:72-7.
- [18] Liu Q, Wu K, Zhu Y, He Y, Wu J, Liu Z. Silencing MAT2A gene by RNA interference inhibited cell growth and induced apoptosis in human hepatoma cells. *Hepatol Res*. 2007; 37:376-88.
- [19] Martínez-Chantar ML, Latasa MU, Varela-Rey M, Lu SC, García-Trevijano ER, Mato JM, et al. L-methionine availability regulates expression of the methionine adenosyltransferase 2A gene in human hepatocarcinoma cells: role of S-adenosylmethionine. *J Biol Chem*. 2003; 278:19885-90.
- [20] Adams R L, Rinaldi A, Seivwright C. Microassay for methyltransferase. *J*

- Biochem Biophys Methods. 1991; 22 : 19-22.
- [21] Pogribny I, Yi P, James SJ. A sensitive new method for rapid of abnormal methylation patterns in global DNA and within CpC islands. *Biochem Biophys Res Commun.* 1999; 262:624-28.
- [22] Chawla RK, Watson WH, Jones DP. Effect of Hypoxia on Hepatic DNA Methylation and tRNA Methyltransferase in Rat: Similarities to Effects of Methyl-Deficient Diets. *Journal of Cellular Biochemistry.* 1996; 61 :72-80 .
- [23] Wainfan, E., Dizik, M., Stender, M., and Christman, J. K. Rapid appearance of hypomethylated DNA in livers of rats fed cancer-promoting. methyl-deficient diets. *Cancer Res.* 1989; 49: 4094-97.
- [24] Chawla RK, Jones DP. Abnormal metabolism of S-adenosyl-L-methionine in hypoxic rat liver. Similarities to its abnormal metabolism in alcoholic cirrhosis. *Biochim Biophys Acta.* 1994; 1199:45-51.
- [25] Metivier R, Penot G, Hubner MR, Reid G, Brand H, Kos M, et al. Estrogen receptor-alpha directs ordered, cyclical, and combinatorial recruitment of cofactors on a natural target promoter. *Cell.* 2003;115, 751–63.
- [26] Shahrzad S, Bertrand K, Minhas K, Coomber BL. Induction of DNA hypomethylation by tumor hypoxia. *Epigenetics.* 2007 ; 2:119-25.
- [27] Poke FS, Qadi A, Holloway AF. Reversing aberrant methylation patterns in cancer. *Curr Med Chem.* 2010;17:1246-54.
- [28] Yao DF, Jiang H, Yao M, Li YM, Gu WJ, Shen YC, et al. Quantitative analysis of hepatic hypoxia-inducible factor-1alpha and its abnormal gene expression during

- the formation of hepatocellular carcinoma. *Hepatobiliary Pancreat Dis Int.* 2009 ; 8:407-13.
- [29] Zhou J, Schmid T, Schnitzer S, Brüne B. Tumor hypoxia and cancer progression. *Cancer Lett.* 2006; 237: 10–21
- [30] Gwak GY, Yoon JH, Kim KM, Lee HS, Chung JW, Gores GJ. Hypoxia stimulates proliferation of human hepatoma cells through the induction of hexokinase II expression. *J Hepatol.* 2005; 42: 358–64.
- [31] Lu SC, Huang ZZ, Yang H, Mato JM, Avila MA, Tsukamoto H. Changes in methionine adenosyltransferase and S-adenosylmethionine homeostasis in alcoholic rat liver. *Am J Physiol Gastrointest Liver Physiol.* 2000; 279:G178-85.
- [32] Hermes M, Osswald H, Mattar J, Kloor D. Influence of an altered methylation potential on mRNA methylation and gene expression in HepG2 cells. *Experimental Cell Research.* 2004; 294: 325– 34.
- [33] Hermes M, von Hippel S, Osswald H, Kloor D. S-adenosylhomocysteine metabolism in different cell lines: effect of hypoxia and cell density. *Cell Physiol Biochem.* 2005;15:233-44
- [34] Ramani K, Yang H, Xia M, Ara AI, Mato JM, Lu SC. Leptin's mitogenic effect in human liver cancer cells requires induction of both methionine adenosyltransferase 2A and 2beta. *Hepatology.* 2008; 47:521-31.
- [35] Yang H, Huang ZZ, Wang J, Lu SC. The role of c-Myb and Sp1 in the up-regulation of methionine adenosyltransferase 2A gene expression in human hepatocellular carcinoma. *FASEB J.* 2001; 15:1507-16.

[36] Martínez-Chantar ML, Latasa MU, Varela-Rey M, Lu SC, García-Trevijano ER, Mato JM, et al. L-methionine availability regulates expression of the methionine adenosyltransferase 2A gene in human hepatocarcinoma cells: role of S-adenosylmethionine. *J Biol Chem.* 2003; 278:19885-90.

Figure Legends

Figure 1. The effect of hypoxia on genomic DNA methylation in Hep3B cells. (A) C-5 MT-ase activity expressed as the amount of incorporated [methyl-³H] groups into poly (dI-dC) in cell homogenates. (B) The methyl-accepting capacity of undigested genomic DNA expressed as the amount of [methyl-³H] groups incorporated into genomic DNA. (C) Methylation-dependent restriction analysis. The amount of genomic DNA that was undigested or digested with HpaII or BssHII was expressed as the number of incorporated methyl groups in DNA. The data were presented as $x \pm s$ for three independent experiments. * $P < 0.05$ vs. control.

Figure 2. Changes in SAM and SAH levels and [³H]-methyl incorporation in xenograft liver tumors. (A) MAT2A and HIF-1 α protein levels in xenograft tumors and cells in culture were determined by Western blot. SAM (B) and SAH (C) levels in xenograft tumors were measured by HPLC. The incorporation of radiolabeled [³H] methyl groups from SAM by DNA isolated from hypoxic xenograft tumors and control cancer cell lines. (D) Radioactivity incorporated in the reaction mediated by HpaII. (E) Radioactivity incorporated in the reaction mediated by SssI. The data were presented as $x \pm s$ for three independent experiments. * $P < 0.05$ vs. control.

Figure 3. MAT2A is transcriptionally regulated by HIF-1 α in Hep3B cells. (A) HCC tissues and their adjacent non-tumor liver tissues were collected and analyzed by immunohistochemistry for MAT2A (a-c) and HIF-1 α (d-f). Representative results were shown for normal liver tissues (a, d) obtained from liver trauma patients undergoing partial hepatectomy, liver cancer tissues (b, e), and peritumoral non-cancerous tissues (c, f). (B) Hep3B cells were transfected as indicated and exposed to hypoxia, the cell lysate was extracted for luciferase assay. Hep3B cells were exposed to hypoxia, and the protein level of MAT2A and HIF-1 α (C) or DNMT1, DNMT3 α and DNMT3 β (D) was determined by Western blot. (E) Hep3B cells were transfected as indicated. After 24 h, the cells were exposed to hypoxia for 24 h or treated with 100 μ mol/L CoCl₂ for 24 h, and the protein level of MAT2A and HIF-1 α was determined by Western blot. β -actin and Histone H3.1 served as loading control for cytoplasmic and nuclear fractions, respectively. Shown were representative blots from three independent experiments with similar results.

Figure 4. Functional characterization of HRE in MAT2A promoter. Hep3B cells were co-transfected with pCMV-HIF-1 α and the pGL3 basic vector or different pGL3 MAT2A promoter reporters under normoxic conditions. The cells were also co-transfected with the pRL-SV40 plasmid to normalize transfection efficiency. (A) At 24 h after transfection, the protein level of HIF-1 α was determined by Western blot. (B) The putative HRE binding sites (with the core sequence of ACGT) at the 5'-flanking region of the MAT2A gene was underlined. (C-E) Luciferase activities were measured using the dual-luciferase reporter assay system. Note the significant induction of luciferase activities driven by the 2.5-kb MAT2A promoter in the cells co-transfected with pCMV-HIF-1 α (C), the significant induction of luciferase activity

driven by the 0.25–0.5-kb (–410/–204) fragment of the human MAT2A promoter (D), and the disrupted induction of luciferase activity by the mutated 0.25–0.5-kb fragment of MAT2A promoter. N: normoxia; HP: hypoxia. Results shown were from three independent experiments. * $p < 0.05$ vs. control.

Figure 5. HIF-1 α binds the consensus HRE motif in MAT2A promoter in hypoxic hepatoma cells. (A) HepG2 cells were cultured under normoxia or hypoxia for 12, 24 or 36 h. Nuclear proteins were harvested, and binding of a consensus HRE oligonucleotide to the MAT2A promoter was analyzed by EMSA. For supershift and competition experiments, extracts from cells cultured for 24 h under hypoxic conditions were used. (B) ChIP assay showing the binding of HIF-1 α to MAT2A promoter in hypoxic Hep3B cells (N: normoxia; HP: hypoxia). (C) Indirect immunofluorescence experiments showing the nuclear translocation of HIF-1 α in hypoxic Hep3B cells. (D) Hep3B cells were cultured under normoxia or hypoxia for 12 and 24 h. Following subcellular fractionation, HIF-1 α protein level in the nuclear and cytoplasmic fractions was determined by Western blot.

Figure 6. Hypoxia-induced MAT2A expression is regulated by HDAC1 and p300. Hep3B cells cultured under hypoxia were treated with TSA (500 nM) or chetomin (100 nM) for 24 h. The cells were lysed for real-time PCR (A) and western blot analysis (B). (C) ChIP assay showing the binding of HIF-1 α to MAT2A promoter in hypoxic Hep3B cells. The re-ChIP assay showing the binding of HDAC1 and p300 to MAT2A promoter in hypoxic Hep3B cells. Shown were representative results from at least four independent experiments. * $p < 0.05$ vs. control.

Figure 1

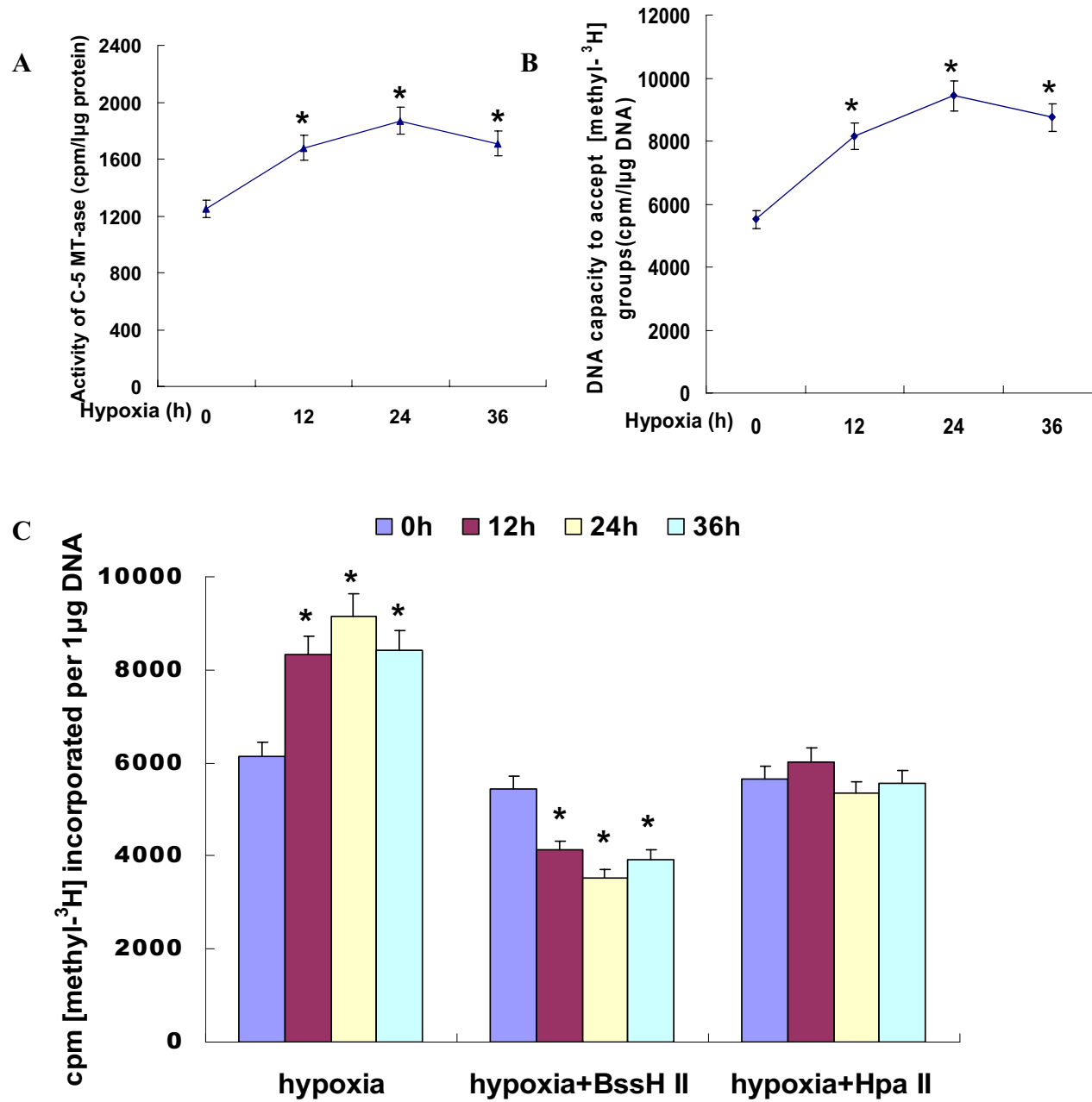


Figure 2

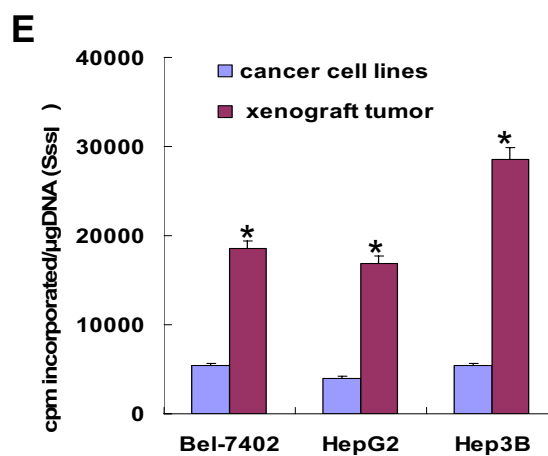
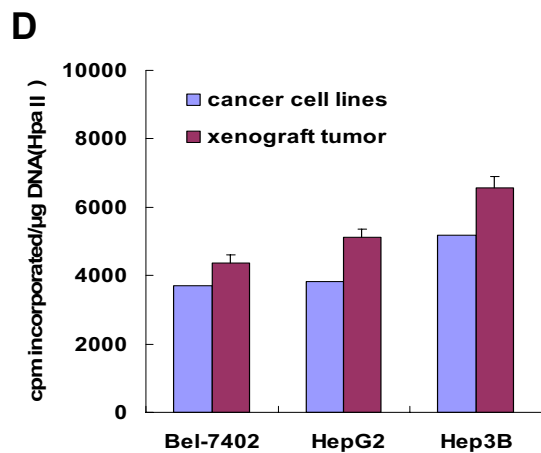
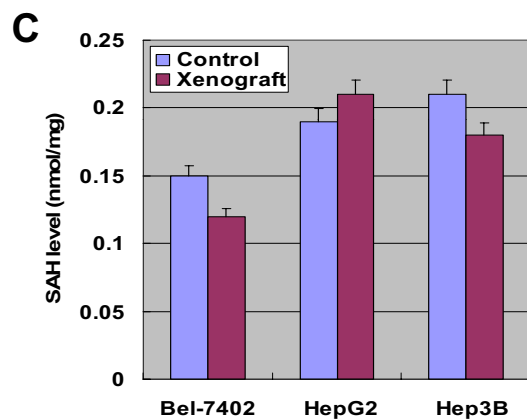
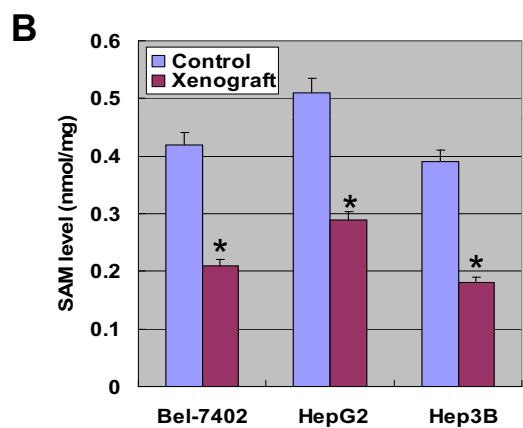
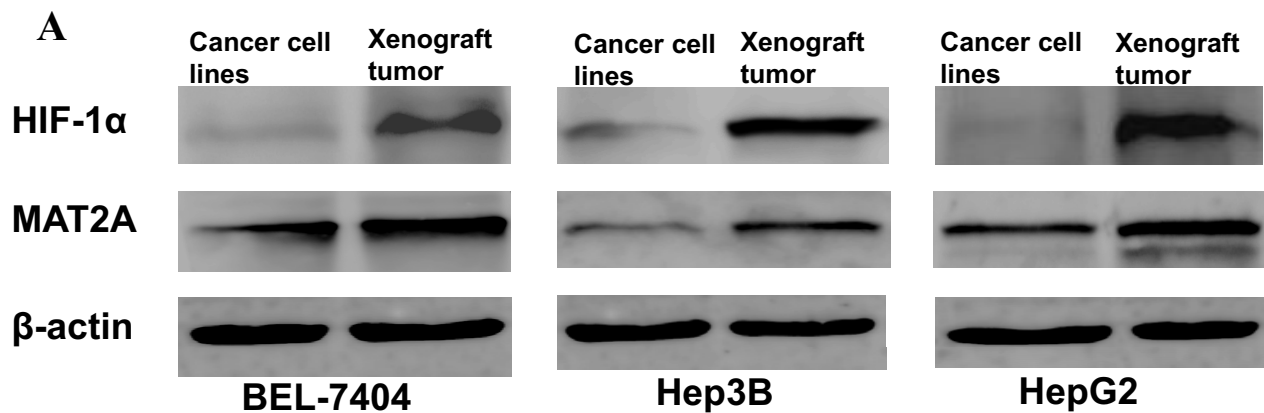
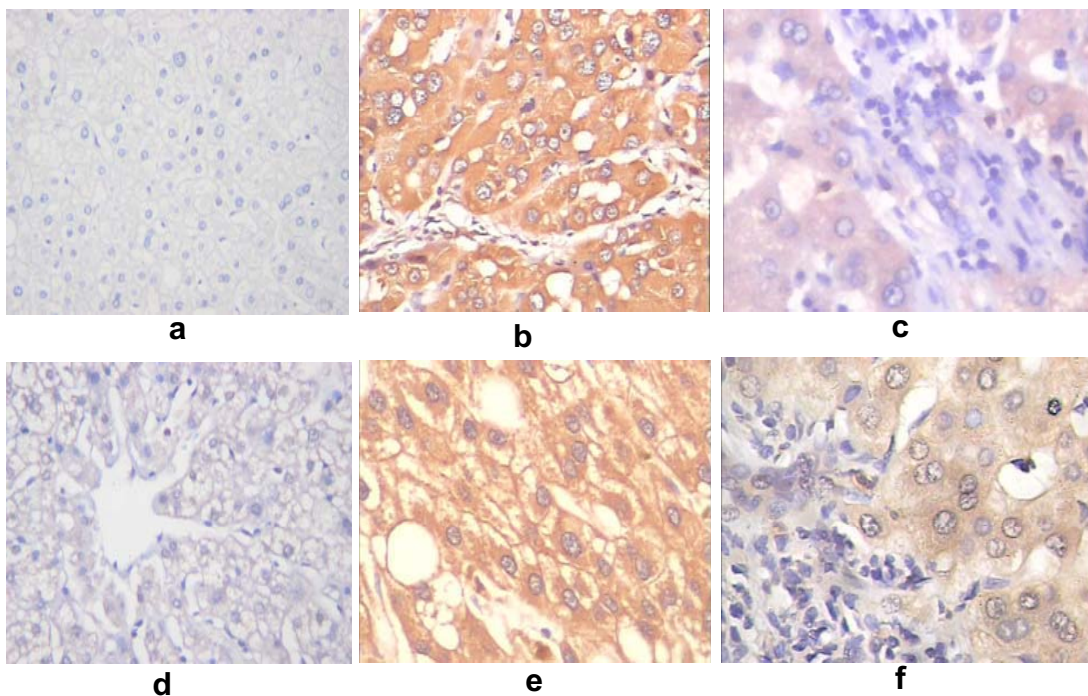
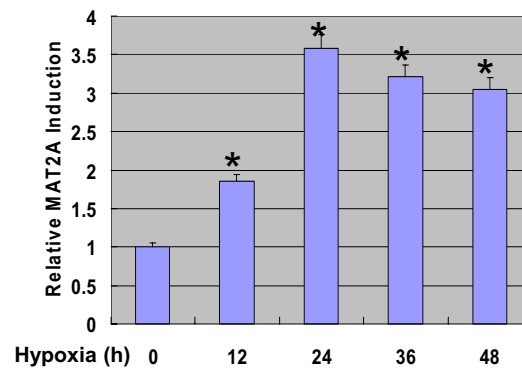


Figure 3

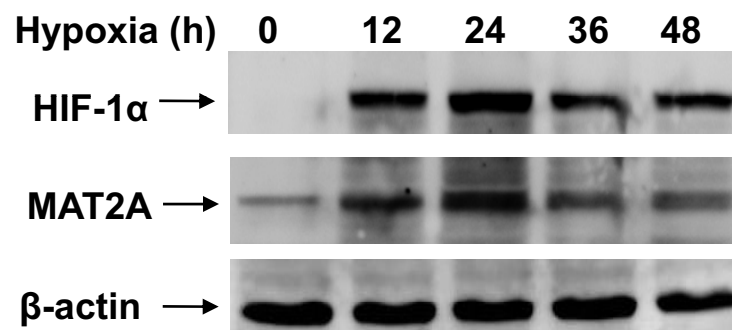
A



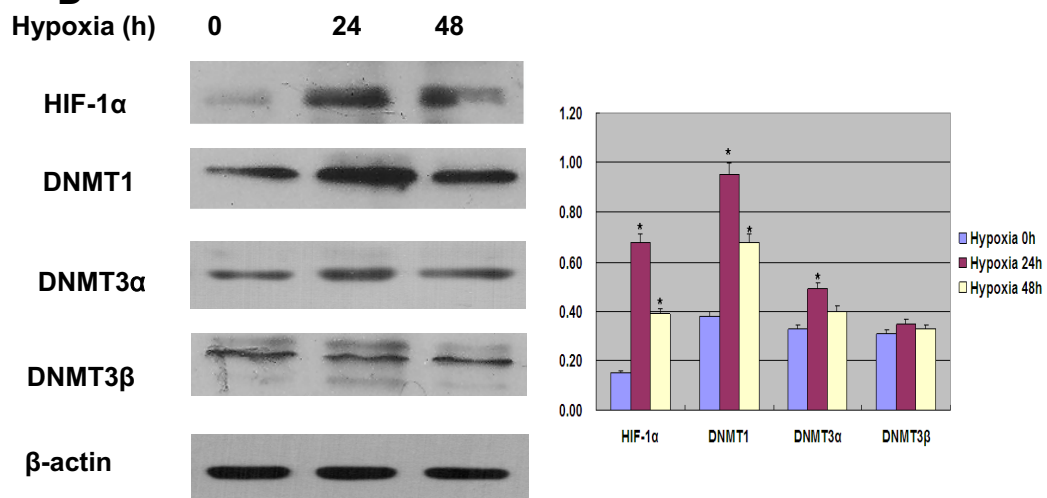
B



C



D



E

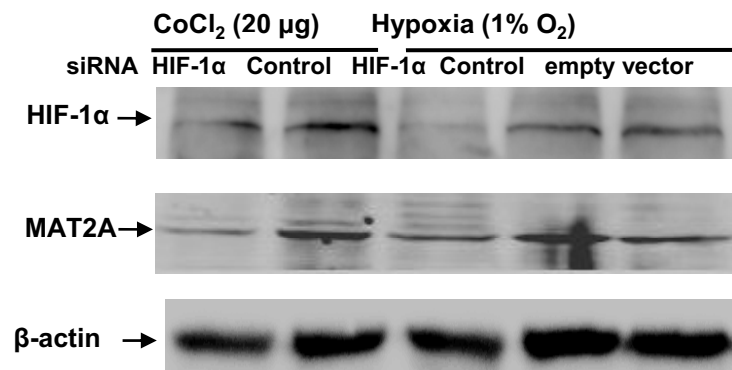


Figure 4

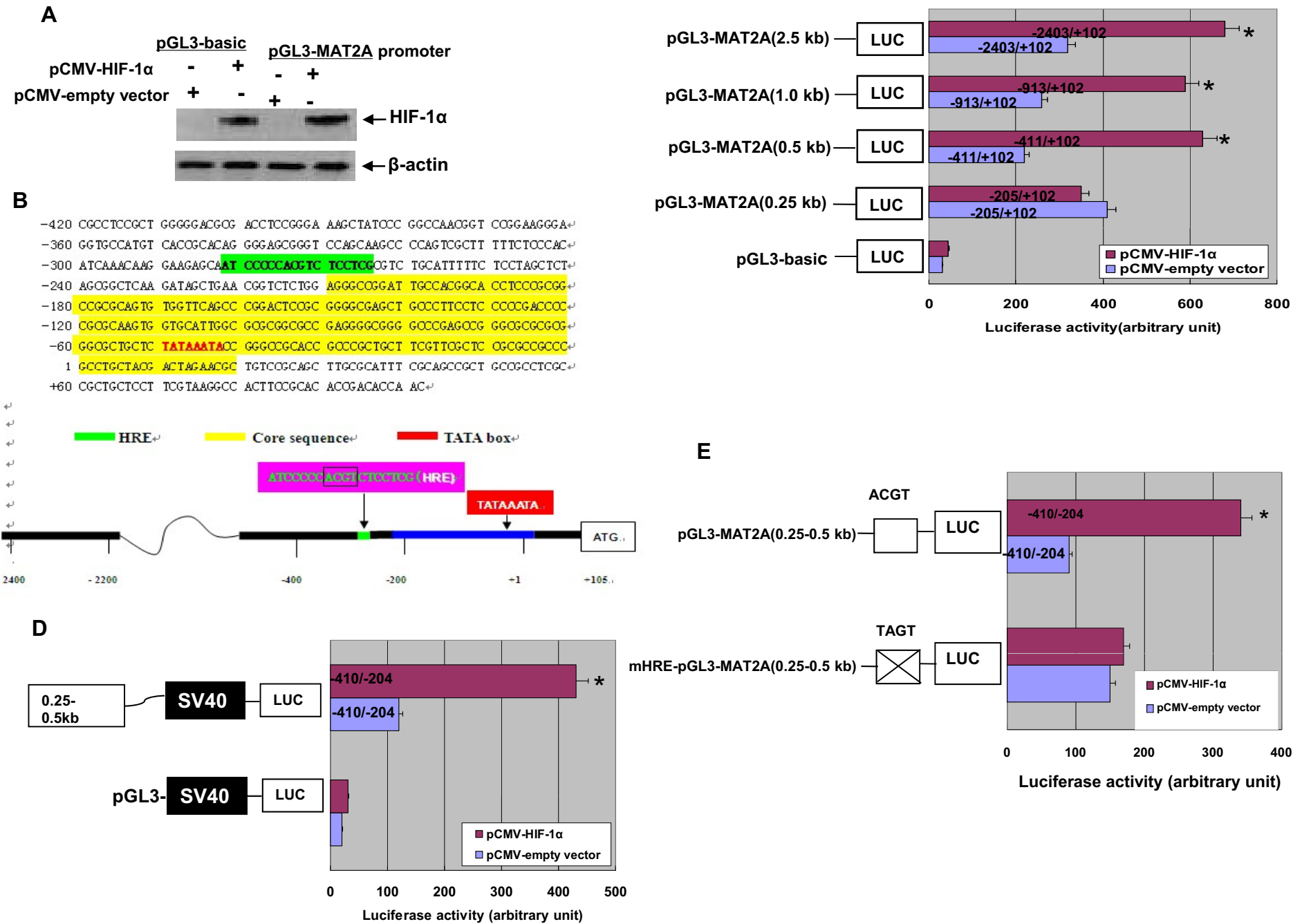
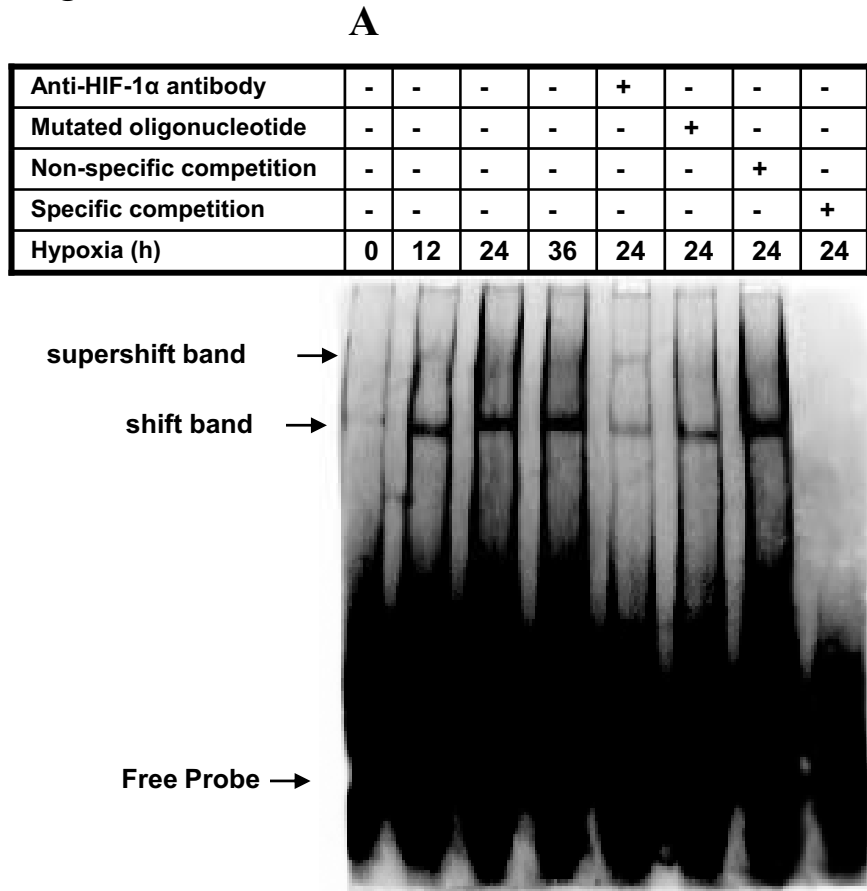
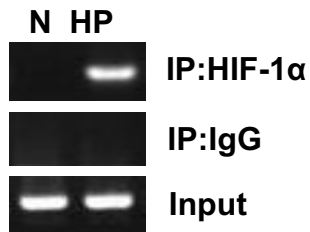


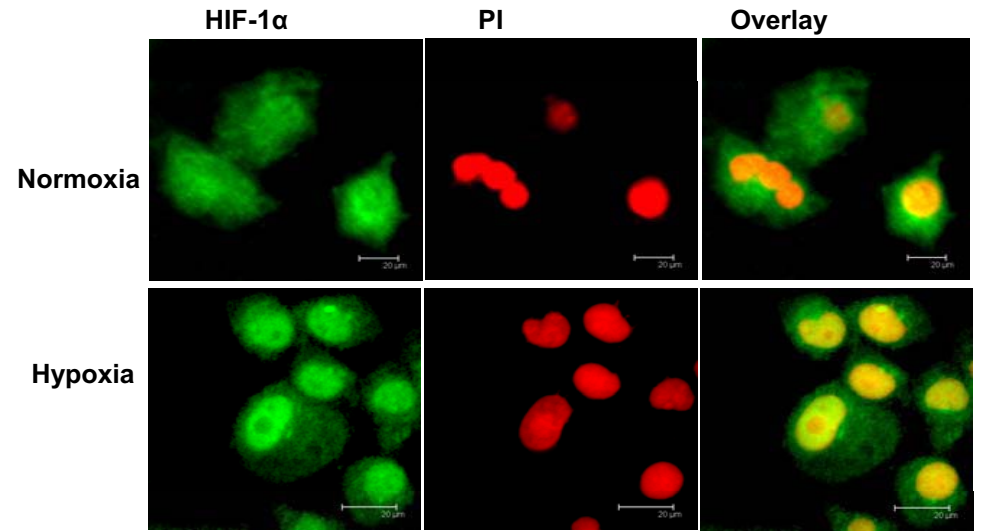
Figure 5



B



C



D

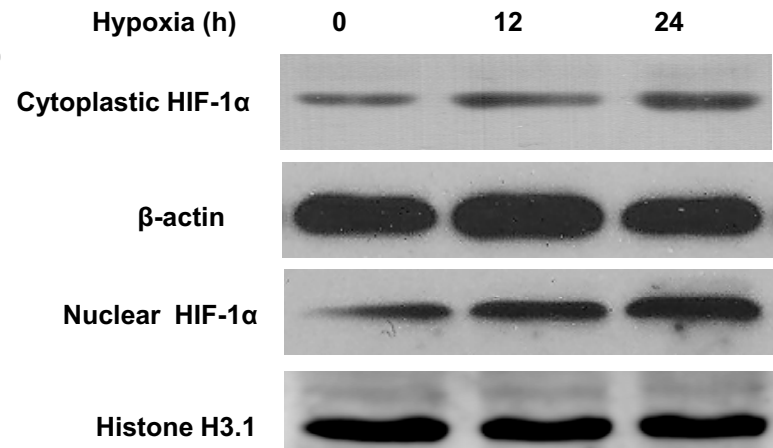
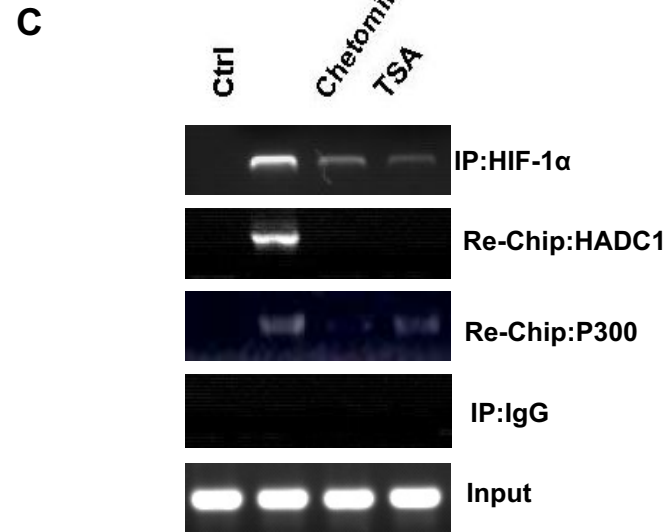
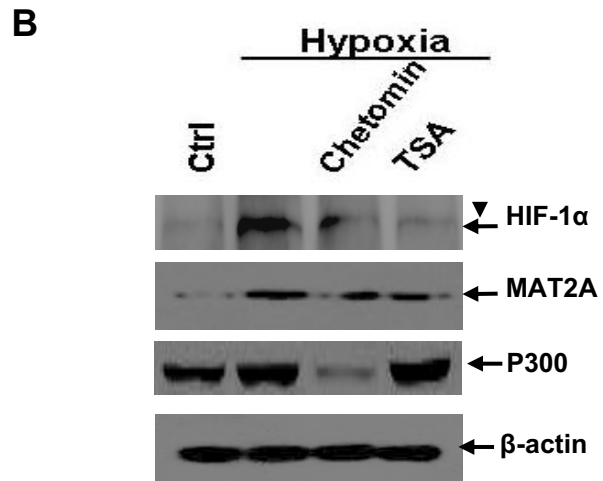
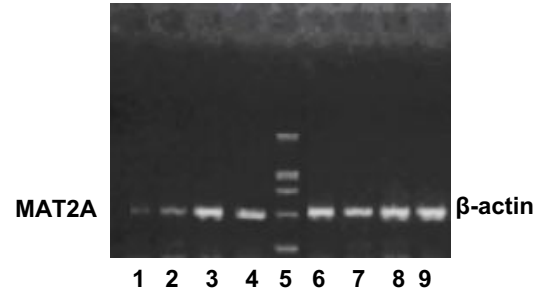
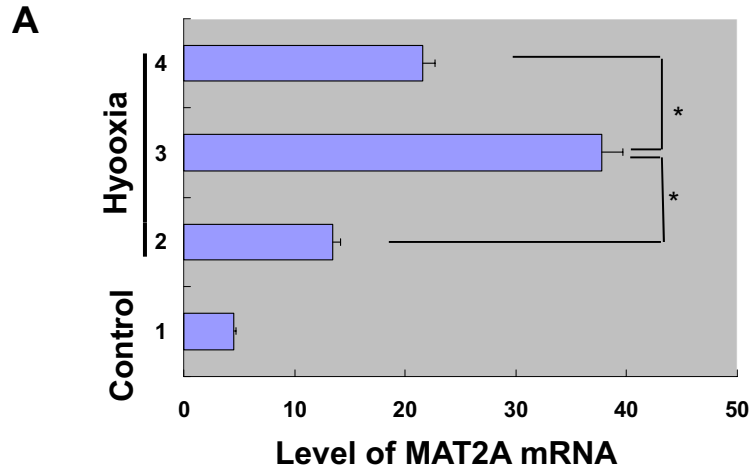


Figure 6



Molecular Cancer Therapeutics

Hypoxia induces genomic DNA demethylation through the activation of HIF-1 α and transcriptional up-regulation of MAT2A in hepatoma cells

Quanyan Liu, Li Liu, Yuhong zhao, et al.

Mol Cancer Ther Published OnlineFirst April 1, 2011.

Updated version	Access the most recent version of this article at: doi: 10.1158/1535-7163.MCT-10-1010
Supplementary Material	Access the most recent supplemental material at: http://mct.aacrjournals.org/content/suppl/2011/04/01/1535-7163.MCT-10-1010.DC1.html
Author Manuscript	Author manuscripts have been peer reviewed and accepted for publication but have not yet been edited.

E-mail alerts	Sign up to receive free email-alerts related to this article or journal.
Reprints and Subscriptions	To order reprints of this article or to subscribe to the journal, contact the AACR Publications Department at pubs@aacr.org .
Permissions	To request permission to re-use all or part of this article, contact the AACR Publications Department at permissions@aacr.org .